

NMR Structural Analysis of MC1R-Targeted Rhenium(II) Metallopeptides and Biological Evaluation of $^{99m}\text{Tc}(\text{I})$ Congeners

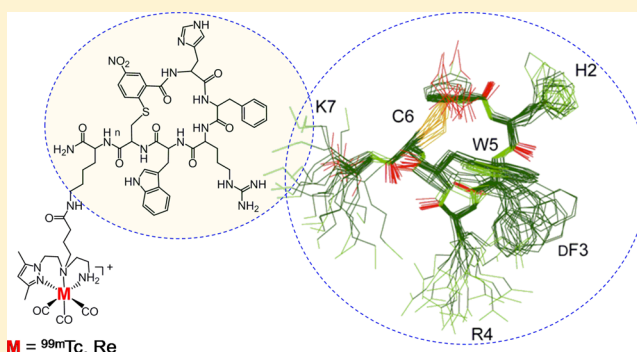
Maurício Morais,[†] Paula D. Raposinho,[†] Maria Cristina Oliveira,[†] David Pantoja-Uceda,[‡] Maria Angeles Jiménez,[‡] Isabel Santos,^{*,†} and João D. G. Correia[†]

[†]Unidade de Ciências Químicas e Radiofarmacêuticas, ITN, Instituto Superior Técnico, Universidade Técnica de Lisboa, Estrada Nacional 10, 2686-953, Sacavém, Portugal

[‡]Instituto de Química Física Rocasolano, Consejo Superior de Investigaciones Científicas (CSIC), Serrano 119, 28006 Madrid, Spain

S Supporting Information

ABSTRACT: The melanocortin receptor 1 (MC1R) is a specific molecular target for detection and therapy of melanoma, as it is overexpressed in human melanomas. The design of novel peptide-based MC1R-specific probes for imaging or targeted radionuclide therapy is being actively pursued. Aiming to visualize melanoma in vivo by single photon emission computed tomography (SPECT) imaging using $^{99m}\text{Tc}(\text{CO})_3$ -labeled cyclic melanocyte stimulating hormone analogues, we have designed the novel cyclic peptides $c[\text{S-NO}_2\text{-C}_6\text{H}_4\text{-CO-His-DPhe-Arg-Trp-Cys}]\text{-Lys-NH}_2$ (**1**) and $c[\text{NH-NO}_2\text{-C}_6\text{H}_3\text{-CO-His-DPhe-Arg-Trp-Lys}]\text{-Lys-NH}_2$ (**2**) and their corresponding conjugates $c[\text{S-NO}_2\text{-C}_6\text{H}_3\text{-CO-His-DPhe-Arg-Trp-Cys}]\text{-Lys(pz)-NH}_2$ (**L1**) and $c[\text{NH-NO}_2\text{-C}_6\text{H}_3\text{-CO-His-DPhe-Arg-Trp-Lys}]\text{-Lys(pz)-NH}_2$ (**L2**), which incorporate a pyrazolyl-diamine chelating unit (pz). Upon reaction with adequate organometallic precursors, we prepared the metalated peptides $c[\text{S-NO}_2\text{-C}_6\text{H}_3\text{-CO-His-DPhe-Arg-Trp-Cys}]\text{-Lys(pz-M}(\text{CO})_3\text{)-NH}_2$ ($M = \text{Re}$ (**Re1**), Tc (**Tc1**)) and $c[\text{NH-NO}_2\text{-C}_6\text{H}_3\text{-CO-His-DPhe-Arg-Trp-Lys}]\text{-Lys(pz-M}(\text{CO})_3\text{)-NH}_2$ ($M = \text{Re}$ (**Re2**), Tc (**Tc2**)). Competitive binding affinity assays demonstrated that metalation of **L1** and **L2** did not lead to a significant decrease of binding affinity toward MC1R, as concluded by comparing the IC_{50} values of **Re1** ($\text{IC}_{50} = 690 \pm 250$ nM) and **Re2** ($\text{IC}_{50} = 176 \pm 5$ nM) to those of the nonmetalated conjugates **L1** ($\text{IC}_{50} = 430 \pm 100$ nM) and **L2** ($\text{IC}_{50} = 179 \pm 39$ nM). Furthermore, the potency of the alkylamine-bridged peptide derivatives is superior to that of the alkylthioaryl-bridged derivatives. NMR structural analysis performed for **1**, **L1**, and **Re1** has shown that the peptide moiety displayed an atypical β -turn conformation in solution. The three-dimensional structural features of the peptide moiety were also conserved upon conjugation to the chelator and, most importantly, after metalation. Despite presenting a significant cell internalization degree and moderate retention in murine melanoma cells, the radiopeptides **Tc1** and **Tc2** displayed poor tumor-targeting properties in a B16F1 melanoma-bearing mouse model.



INTRODUCTION

Among the five subtypes of human melanocortin receptors (hMC1-5R), hMC1R has been explored as a specific molecular target for detection and therapy of melanoma, which accounts for more than 50% of all skin cancer deaths.¹ Indeed, both melanotic and amelanotic murine and human melanomas overexpress the MC1R, and it has been identified in more than 80% of human metastatic melanoma samples.² Unless primary melanoma is detected early enough to be surgically removed, the prognosis of the disease is poor due to the ineffective treatments for fighting a tumor with high metastasizing potential.³ Therefore, the development of peptide-based MC1R-specific probes for single photon emission computed tomography (SPECT) imaging (γ emitters), positron emission tomography (PET) imaging (β^+ emitters) or targeted radionuclide therapy (β^- or α particles) is a subject of great interest and intense research.^{1a,2,4}

α -Melanocyte stimulating hormone (α -MSH), a tridecapeptide (Figure 1), is the most potent naturally occurring

melanotropic peptide for the activation of MC1R but presents a short half-life in vivo.⁵ Replacement of Met⁴ and Phe⁷ by Nle and DPhe, respectively, gave the analogue [Nle⁴,DPhe⁷]- α -MSH (NDP- α -MSH), which presented greater metabolic stability and improved potency in comparison to α -MSH.⁵

Following the structure–bioactivity relationship studies of different linear and cyclic α -MSH analogues, it has been concluded that the central sequence of α -MSH, His⁶-Phe⁷-Arg⁸-Trp⁹, is required for receptor recognition.⁵ These efforts led to the discovery of the shorter and more rigid and potent cyclic analogue Ac-Nle⁴-c[Asp⁵-His⁶-DPhe⁷-Arg⁸-Trp⁹-Lys¹⁰]-NH₂ (MT-II) (Figure 2),⁶ which has been also used as a model for the design of potent antagonists such as

Special Issue: Organometallics in Biology and Medicine

Received: June 6, 2012

Published: August 3, 2012

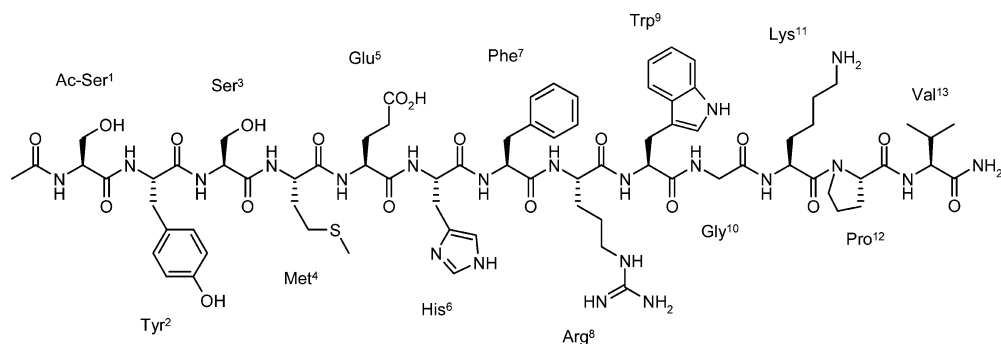


Figure 1. Structure of α -Melanocyte stimulating hormone (α -MSH).

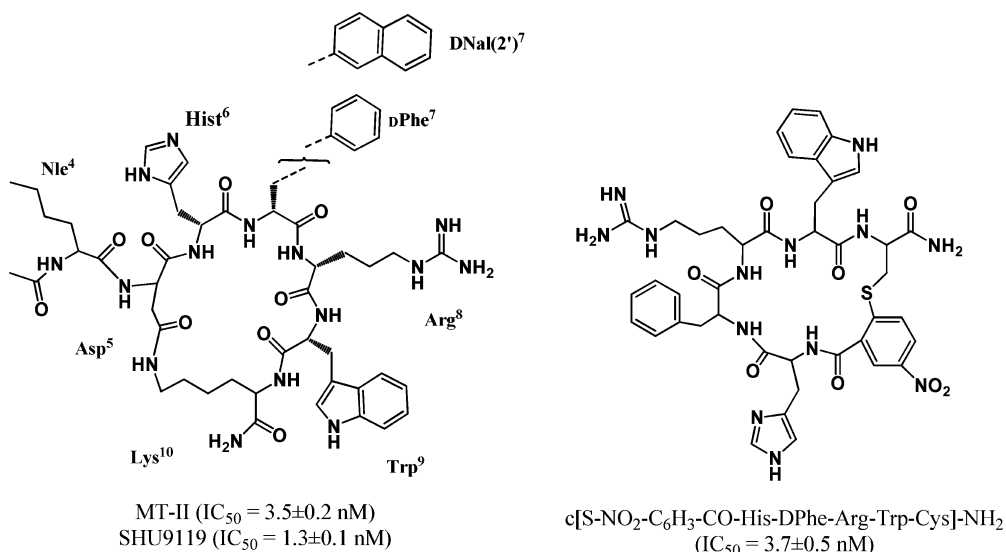


Figure 2. Structural formulas of the cyclic analogues MT-II, SHU9119, and $c[S-NO_2-C_6H_3-CO-His-DPhe-Arg-Trp-Cys]-NH_2$ (PG10N).

Ac-Nle⁴- $c[Asp^5-His^6-DNaI(2')^7Arg^8-Trp^9-Lys^{10}]-NH_2$ (SHU-9119) (Figure 2).⁷

Recently, Grieco et al. have synthesized and characterized pharmacologically a new family of alkylthioaryl-bridged macrocyclic peptides formally derived from MT-II and SHU9119.⁸ The analogue $c[S-NO_2-C_6H_3-CO-His-DPhe-Arg-Trp-Cys]-NH_2$ (PG10N) exhibited potent full agonist activity at hMC1R, hMC3R, hMC4R, and hMCR5 (Figure 2).

Considering our interest in the design of MC1R-targeting cyclic α -MSH analogues for melanoma imaging, we now report on the synthesis and characterization of the novel 19- and 22-membered macrocyclic peptides $c[S-NO_2-C_6H_3-CO-His-DPhe-Arg-Trp-Cys]-Lys-NH_2$ (**1**) and $c[NH-NO_2-C_6H_3-CO-His-DPhe-Arg-Trp-Lys]-Lys-NH_2$ (**2**), respectively, and on their pyrazolyl-diamine conjugates $c[S-NO_2-C_6H_3-CO-His-DPhe-Arg-Trp-Cys]-Lys(pz)-NH_2$ (**L1**) and $c[NH-NO_2-C_6H_3-CO-His-DPhe-Arg-Trp-Lys]-Lys(pz)-NH_2$ (**L2**) (Figure 3). We will also describe the $Re(CO)_3$ -metalated peptides **Re1** and **Re2**, as well as the MC1R-targeting properties of the ^{99m}Tc congeners **Tc1** and **Tc2**. To assess whether conjugation to the chelator and subsequent metalation affected the structural behavior of α -MSH analogues, structural analysis by NMR was performed for the 19-membered macrocyclic analogues.

RESULTS AND DISCUSSION

Synthesis of the Peptide Conjugates. In the past few years we have introduced tridentate bifunctional chelators

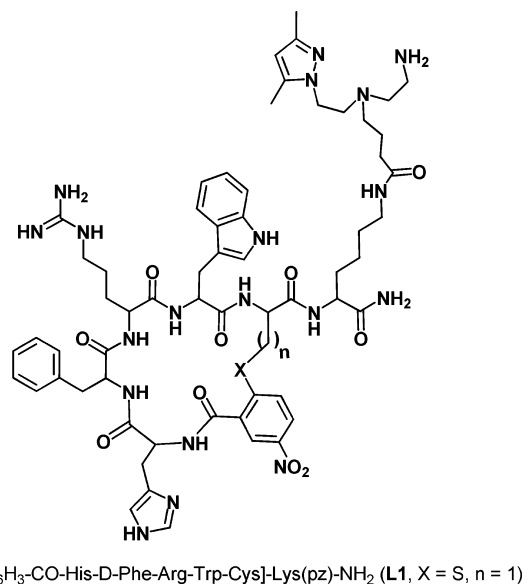


Figure 3. Structural formulas of the macrocyclic peptide conjugates **L1** and **L2**.

(BFC's) that combine a pyrazolyl unit with amines, carboxylates, and/or thioethers for stabilization of the *fac*- $[M(CO)_3]^+$ core ($M = ^{99m}Tc, Re$).⁹ Some of these BFC's have been conjugated to

a wide variety of biologically relevant peptides (e.g., bombesin and α -MSH analogues) through a pendant carboxylate arm, allowing their labeling in high radiochemical yield and high specific activity.¹⁰ With the aim of applying the same strategy to the MT-II analogues proposed herein, we have designed new peptide sequences containing a C-terminal Lys residue to allow conjugation to the BFC (Figure 3).

We started with the synthesis of the macrocyclic peptides $c[S\text{-NO}_2\text{-C}_6\text{H}_3\text{-CO-His-DPhe-Arg-Trp-Cys}]\text{-Lys-NH}_2$ (**1**) and $c[\text{NH-NO}_2\text{-C}_6\text{H}_3\text{-CO-His-DPhe-Arg-Trp-Lys}]\text{-Lys-NH}_2$ (**2**) using the three-step procedure described by Grieco et al.^{8,11} Briefly, after the linear peptide intermediates were assembled in a microwave-assisted solid-phase peptide synthesizer using the Fmoc strategy, the peptides were capped with 2-fluoro-5-nitrobenzoic acid and the Trt or Mtt protecting groups of Cys or Lys, respectively, were removed with a dilute solution of trifluoroacetic acid (TFA). Cyclization, through an aromatic nucleophilic substitution mechanism, was achieved by treating the resin-supported peptides with potassium carbonate in DMF (36 h at 25 °C). The resulting macrocyclic peptides **1** and **2** were cleaved from the resin under standard conditions, precipitated with diethyl ether, and purified by semipreparative reverse-phase high-performance liquid chromatography (RP-HPLC). Conjugation of the Boc-protected pyrazolyl-diamine (pz) BFC to the ϵ -amino group of the C-terminal Lys in **1** and **2**, followed by Boc deprotection and purification by RP-HPLC, yielded the peptide conjugates $c[S\text{-NO}_2\text{-C}_6\text{H}_3\text{-CO-His-DPhe-Arg-Trp-Cys}]\text{-Lys-(pz)-NH}_2$ (**L1**) and $c[\text{NH-NO}_2\text{-C}_6\text{H}_3\text{-CO-His-DPhe-Arg-Trp-Lys}]\text{-Lys-(pz)-NH}_2$ (**L2**), respectively (Figure 3). Peptides **1** and **2** and the final conjugates **L1** and **L2** were characterized by electrospray ionization–mass spectrometry (ESI-MS) (Table 1).

Table 1. Analytical Data for 1, 2, L1, L2, Re1, and Re2

compd	formula	mass, m/z		t_R^a , min (>98% purity)
		calcd [ion]	found	
1	C ₄₈ H ₅₉ N ₁₅ O ₉ S	1022.4 [M + H] ⁺	1022.5	9.1
L1	C ₆₁ H ₈₁ N ₁₉ O ₁₀ S	1272.5 [M + H] ⁺	1272.5	10.2
Re1	C ₆₄ H ₈₄ N ₁₉ O ₁₃ ReS	772.4 [M + 2H] ²⁺	772.4	11.9
2	C ₅₁ H ₆₆ N ₁₆ O ₉	1047.5 [M + H] ⁺	1047.5	9.3
L2	C ₆₄ H ₈₈ N ₂₀ O ₁₀	1297.7 [M + H] ⁺	1297.7	10.4
Re2	C ₆₇ H ₉₁ N ₂₀ O ₁₃ Re	784.4 [M + 2H] ²⁺	784.4	12.1

^aSee Materials and Methods for HPLC analytical conditions.

Aiming to assess the influence of metalation in the MC1R-binding affinity and to further characterize the radioactive complexes, we have synthesized the “cold” rhenium surrogates $c[S\text{-NO}_2\text{-C}_6\text{H}_3\text{-CO-His-DPhe-Arg-Trp-Cys}]\text{-Lys-(pz-Re-(CO)}_3\text{)-NH}_2$ (**Re1**) and $c[\text{NH-NO}_2\text{-C}_6\text{H}_3\text{-CO-His-DPhe-Arg-Trp-Lys}]\text{-Lys-(pz-Re-(CO)}_3\text{)-NH}_2$ (**Re2**) by conjugation of the free carboxylate group in the precursor $fac\text{-[Re(CO)}_3\text{(k}^3\text{-pz-CO}_2\text{H)]}^+$ to the Lys residue of **1** and **2**, respectively, using standard coupling reagents (Scheme 1). The metalated peptides **Re1** and **Re2** were purified by semipreparative RP-HPLC and characterized by ESI-MS (Table 1).

Determination of the MC1R Binding Affinities. The binding affinities of the cyclic α -MSH analogues to MC1R were tested in a competitive binding assay using [¹²⁵I]-NDP- α MSH as radioligand and murine melanoma B16F1 cells. The calculated

IC₅₀ values for **L1/L2** and **Re1/Re2** as well as for the precursors **PG10N**, **1**, and **2** are given in Table 2.

The introduction of an additional Lys residue at the C terminus of the alkylthioaryl-bridged macrocyclic peptide $c[S\text{-NO}_2\text{-C}_6\text{H}_3\text{-CO-His-DPhe-Arg-Trp-Cys}]\text{-NH}_2$ (**PG10N**) led to the analogue **1**, which is 486-fold less potent than the parent peptide (Table 2). Replacement of the alkylthioaryl bridge in **1** by an alkylaminoaryl bridge gave the 22-membered macrocyclic peptide **2**, which is about 10-fold less potent than **PG10N** but considerably more potent than peptide **1** (Table 2).

Conjugation of the BFC to peptide **1** led to an improvement of the binding affinity of the resulting peptide conjugate **L1**; however, it is still 100-fold less potent than the parent peptide **PG10N** (Table 2).

Unlike peptide **1**, the MC1R binding affinity of peptide **2** decreases upon conjugation to the BFC, since the resulting conjugate **L2** is 4-fold less potent (Table 2).

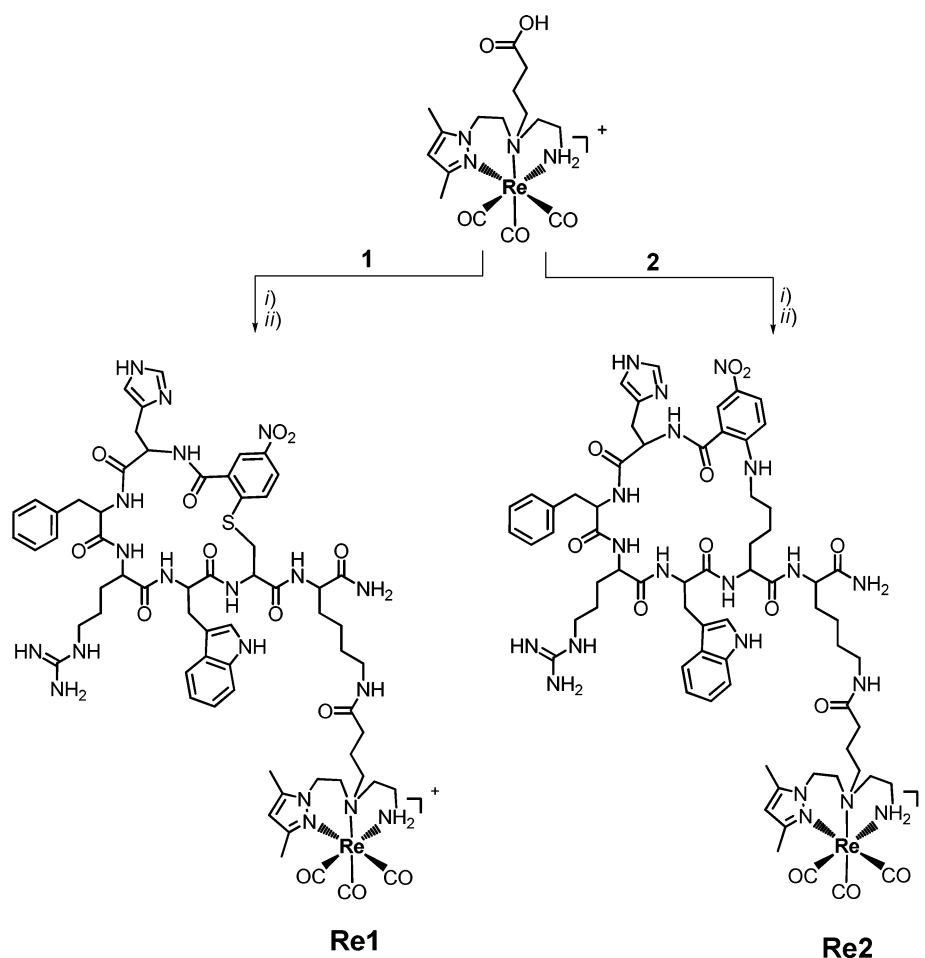
The metalation of **L1** and **L2** with the organometallic core $fac\text{-[Re(CO)}_3\text{)]}^+$ does not lead to a significant decrease of binding affinity toward MC1R, as concluded by comparing the IC₅₀ values of **Re1** (IC₅₀ = 690 ± 250 nM) and **Re2** (IC₅₀ = 176 ± 5 nM) with those of the nonmetalated conjugates (**L1**, IC₅₀ = 430 ± 100 nM) and (**L2**, IC₅₀ = 179 ± 39 nM), respectively (Table 2).

Brought together, the binding affinity results show that conjugation of the BFC to the cyclic peptides may lead to conjugates with higher or lower affinity toward MC1R, as is the case of the 19-membered (**L1**) and/or the 22-membered macrocyclic peptide conjugates (**L2**), respectively. However, the most interesting finding is related to the fact that metalation of the peptide conjugates did not affect binding at MC1R, as concluded by comparing the IC₅₀ values of **L1** and **L2** to those of the respective complexes **Re1** and **Re2**. These observations prompted us to experimentally analyze the structural factors that may affect the MC1R interaction properties of the parent peptides, conjugates, and metalated peptides. To that end, we have performed NMR structural studies with the family of the alkylthioaryl-bridged macrocyclic peptides (**1**, **L1**, and **Re1**) in aqueous solution.

NMR Structural Characterization. Once the NMR spectra of the peptides **1**, **L1**, and **Re1** were assigned (see Materials and Methods), the most remarkable finding was that the majority of the ¹H, ¹³C, and ¹⁵N chemical shifts of **L1** and **Re1** are practically identical; they are also nearly identical with those of **1** (Figure 4 and Tables ST1–ST3 (Supporting Information)). The largest differences in chemical shift correspond, as expected, to the Lys side chain to which the chelator is conjugated (Figure 3) and to the very sensitive HN protons, which even so change less than 0.05 ppm between **1** and the conjugate **L1**. In contrast to the case for **1** and **L1**, the metalated peptide **Re1** exhibits two sets of signals for some protons (Figure 4 and Tables ST3 and ST4 (Supporting Information)), which indicates the coexistence of two isomeric species, **Re1a** and **Re1b**, as previously reported for other peptide conjugates metalated with Re.¹² On the basis of the volume integration of TOCSY signals, the two isomers are almost equally populated (53 and 47% at 5 °C and 51 and 49% at 25 °C). Interestingly, the peptide moiety shows similar conformational behavior in the two species, as derived from the examined NMR parameters (see below).

The fact that the chemical shifts for some residues deviate significantly from the random coil values in the three macrocyclic peptides **1**, **L1**, and **Re1** shows that they adopt ordered conformations in aqueous solution. In particular, the chemical shift deviations ($\Delta\delta = \delta^{\text{observed}} - \delta^{\text{random coil}}$ ppm) observed for the ¹H _{ω} , ¹³C _{ω} and ¹³C _{β} backbone atoms, which lie clearly out of the random coil range (Figures SF1–SF2 (Supporting Information)), are

Scheme 1. Synthesis of $c[S\text{-NO}_2\text{-C}_6\text{H}_3\text{-CO-His-DPhe-Arg-Trp-Cys}]\text{-Lys(pz-Re(CO)}_3\text{)-NH}_2$ (**Re1**) and $c[\text{NH-NO}_2\text{-C}_6\text{H}_3\text{-CO-His-DPhe-Arg-Trp-Lys}]\text{-Lys(pz-Re(CO)}_3\text{)-NH}_2$ (**Re2**)^a



^aLegend: (i) DMF/DIPEA/HATU; (ii) TFA/TIS/H₂O.

Table 2. MC1R Binding Affinities of Cyclic α -MSH Analogues

peptide analogue	*IC ₅₀ (nM)
$c[S\text{-NO}_2\text{-C}_6\text{H}_3\text{-CO-His-DPhe-Arg-Trp-Cys}]\text{-NH}_2$ (PG10N) ^s	3.7 ± 0.5
$c[S\text{-NO}_2\text{-C}_6\text{H}_3\text{-CO-His-DPhe-Arg-Trp-Cys}]\text{-Lys-NH}_2$ (1)	1770 ± 480
$c[S\text{-NO}_2\text{-C}_6\text{H}_3\text{-CO-His-DPhe-Arg-Trp-Cys}]\text{-Lys(pz)-NH}_2$ (L1)	430 ± 60
$c[S\text{-NO}_2\text{-C}_6\text{H}_3\text{-CO-His-DPhe-Arg-Trp-Cys}]\text{-Lys(pz-Re(CO)}_3\text{)-NH}_2$ (Re1)	690 ± 250
$c[\text{NH-NO}_2\text{-C}_6\text{H}_3\text{-CO-His-DPhe-Arg-Trp-Lys}]\text{-Lys-NH}_2$ (2)	51 ± 12
$c[\text{NH-NO}_2\text{-C}_6\text{H}_3\text{-CO-His-DPhe-Arg-Trp-Lys}]\text{-Lys(pz)-NH}_2$ (L2)	179 ± 39
$c[\text{NH-NO}_2\text{-C}_6\text{H}_3\text{-CO-His-DPhe-Arg-Trp-Lys}]\text{-Lys(Pz-Re(CO)}_3\text{)-NH}_2$ (Re2)	176 ± 5

indicative of turnlike conformations at the core residues DPhe, Arg, and Trp. Among the side-chain protons, the very large upfield shifts observed for Arg (Table 3) indicate that these side-chain protons bear anisotropic effects from the ring currents of one or more aromatic side chains, as confirmed in the calculated structures (see below). The increase observed for the ¹H chemical shift deviations at 5 °C relative to 25 °C for the three peptides (**1**, **L1**, and **Re1**; Table 3 and Tables ST1-ST3 (Supporting Information)) indicates that the structure adopted by peptide **1** and by the peptide moiety in the peptide conjugates **L1** and **Re1** stabilizes at low temperature.

Further and clear-cut evidence about the family of peptides **1**, **L1**, and **Re1** adopting ordered conformations came from the

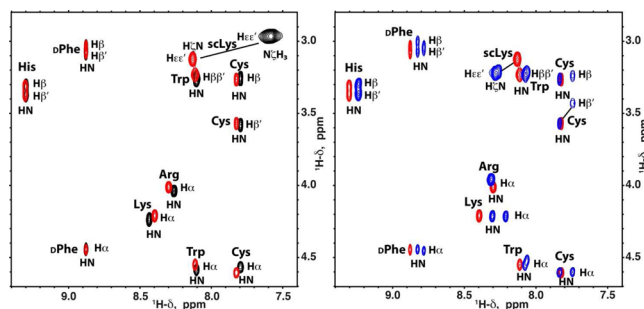


Figure 4. 2D ¹H, ¹H-TOCSY spectral region showing H_α/H_β-HN cross-peaks observed for peptides **1** (black contours), **L1** (red contours), and **Re1** (blue contours) in aqueous solution (H₂O/D₂O 9/1 v/v) at pH 2.5 and 5 °C. The cross-peaks between the H_{εε'} protons and the amino group of the Lys side chain (sCLys) in peptide **1** and the corresponding H_εN amide to which the chelator is bound in the peptide conjugates **L1** and **Re1** are also shown.

NOE/ROE cross-peaks observed in the NOESY spectra at 5 °C and/or ROESY spectra at 25 °C (Figure 5), in particular, by the nonsequential NOE/ROEs (Table ST5 (Supporting Information)). A NOE/ROE between two protons is only observed when they are spatially close. As expected from the similarity in chemical shifts, the peptide moiety in conjugate **L1** and **Re1** exhibits essentially the same set of NOEs as peptide **1** (Figure 5 and Table ST5) and,

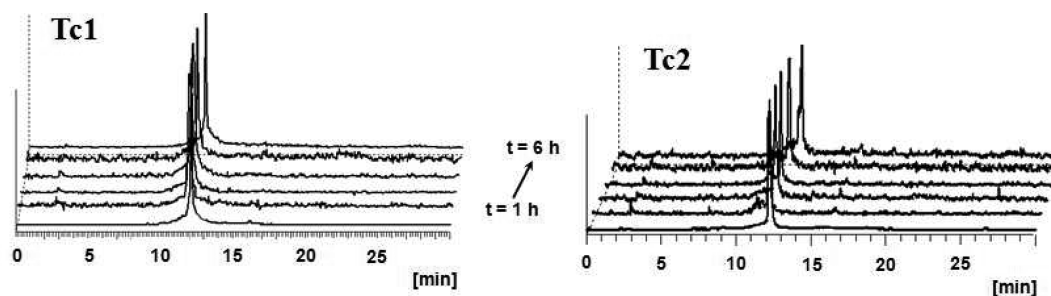


Figure 7. RP-HPLC profiles of Tc1 and Tc2 in fresh human plasma at different time points at 37 °C.

and the Arg side chain is shielded in peptide 1 but not in MTII and VJH085. These structural differences can be explained by the cycle size, which is smaller in peptide 1, PG10N, and [C₅C₁₀]NDP-MSH₅₋₁₀ than in MTII and VJH085.^{8,14,15} It seems that the differences in the cycle size translate into different arrangements of the side chains in the α -MSH analogues, which evidently affects their binding affinity to the receptor. Thus, the difference in cycle size might also account for the differences in affinity found for peptide 1 relative to peptide 2 (Table 2).

Coming back to the 19-membered macrocyclic peptides 1, L1, and Re1, the peptide moiety in L1 and Re1 adopts the same structure as in peptide 1. Hence, the MC1R-binding properties of these compounds are modulated by other factors apart from the conformation of the peptide moiety.

Labeling of the Peptide Conjugates with *fac*-[^{99m}Tc(CO)₃]⁺. The radioactive complexes *c*[S-NO₂-C₆H₃-CO-His-DPhe-Arg-Trp-Cys]-Lys(pz-^{99m}Tc(CO)₃)-NH₂ (Tc1) and *c*[NH-NO₂-C₆H₃-CO-His-DPhe-Arg-Trp-Lys]-Lys(pz-^{99m}Tc(CO)₃)-NH₂ (Tc2), structural analogues of Re1 and Re2, were obtained in almost quantitative yield (>98%) upon reaction of the precursor [^{99m}Tc(CO)₃(H₂O)₃]⁺ with the respective peptide > conjugates L1 and L2 (final concentration (5–8) × 10⁻⁵ M, at 98 °C). With the aim of increasing the specific activity of the ^{99m}Tc-labeled peptides to maximize their MC1R-binding ability, the radiopeptides were separated from the free peptide conjugates by semipreparative RP-HPLC. The fractions corresponding to the radioconjugate were collected in Falcon vials containing PBS for biodistribution studies and cell internalization studies. The purity/stability of the radioconjugates was evaluated by RP-HPLC and ITLC. It has been found that no oxidation or colloid formation took place under those conditions, and only one species was observed by HPLC and ITLC. Further stability assays in fresh human serum at 37 °C indicated that Tc1 and Tc2 have high plasma stability, with negligible enzymatic degradation, even after 6 h of incubation (Figure 7).

We have determined the partition coefficients of Tc1 and Tc2 under physiological conditions to assess their hydro-/lipophilic nature. The results, displayed in Table 5, have shown that all radiopeptides present a moderate hydrophilic character.

Table 5. Retention Time (RP-HPLC) and log *P*_{o/w} Values for Radiopeptides Tc1 and Tc2

complex	<i>t</i> _R min (purity, %)	log <i>P</i> _{o/w} ± SD
Tc1	12.2 (98)	-0.34 ± 0.03
Tc2	12.3 (98)	-0.8 ± 0.05

The identification/characterization of Tc1 and Tc2 was accomplished by comparing their γ traces with the UV-vis traces of the respective rhenium compounds Re1 and Re2 (Figure 8).

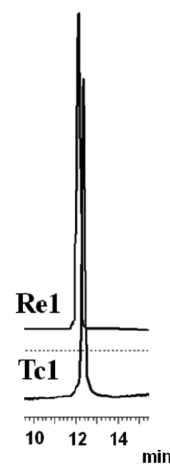


Figure 8. RP-HPLC chromatographic profiles for Tc1 (γ detection) and its respective cold surrogate Re1 (UV-vis detection).

Cell Internalization Studies. The degree of internalization and retention of Tc1 and Tc2 in B16F1 murine melanoma cells is an important parameter for partial prediction of their tumor-targeting properties in vivo. The internalization studies have shown that cellular uptake was time-dependent for both radiopeptides at 37 °C, as displayed in Figure 9.

High to moderate cellular uptake was attained for both radiopeptides, with Tc1 presenting the highest internalization level at 3 h p.i., when ca. 10% of the total applied radioactivity was internalized by the cells. Despite presenting a lower internalization degree, the radiopeptide Tc2 still presented a significant internalization (ca. 5% at 3 h p.i.), comparable to that of previously described ^{99m}Tc(CO)₃-labeled α -MSH analogues.^{10c} With regard to the radioactivity associated with the membrane (surface bound), only a small difference was observed between the two radiopeptides, with Tc1 and Tc2 reaching maximum values at 4 h (14.3%) and 2 h (12.3%) post incubation, respectively.

The cellular retention of the radioconjugates was also evaluated in the same cell line at different time points (Figure 10). A moderate and similar retention was observed for Tc1 and Tc2, with ca. 50% of the cell-associated activity still remaining inside the cells after 2 h.

Brought together, the significant cell internalization degree and the moderate retention of Tc1 and Tc2 in murine melanoma cells prompted us to assess the tumor-targeting properties of those radiopeptides in a B16F1 melanoma-bearing mouse model. Biodistribution studies of the radiopeptides Tc1 and Tc2 in B16F1 melanoma-bearing mice at 1 and 4 h after intravenous injection are summarized in Table 6.

Despite the high in vivo stability in blood and urine, biological evaluation of new cyclic radioconjugates in melanoma-bearing mice correlated well with the low affinity for the MC1R, as

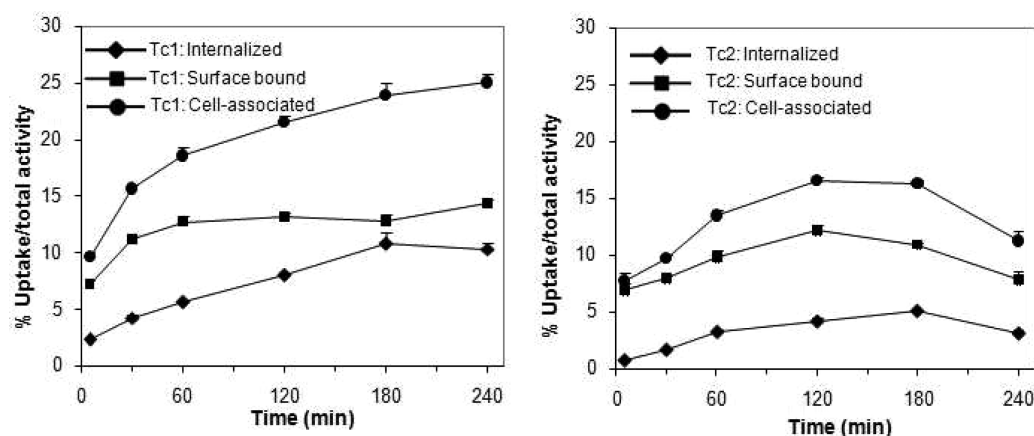


Figure 9. Internalization of Tc1 and Tc2 in B16F1 cells at different time points at 37 °C. Internalized and surface-bound activities are expressed as a percentage of applied activity.

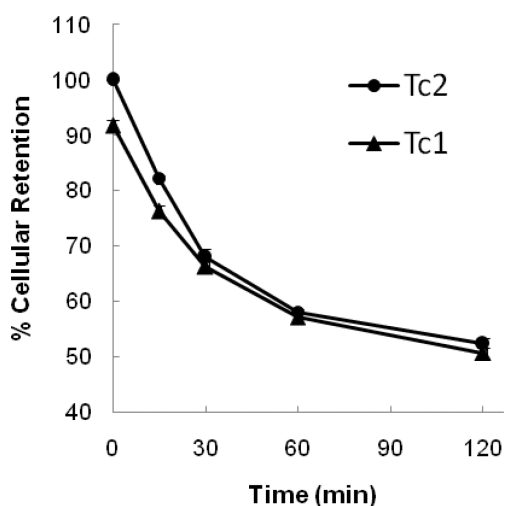


Figure 10. Cellular retention of internalized Tc1 and Tc2 radiopeptides in B16F1 cells at different time points at 37 °C.

evidenced by the low tumor uptake values found for Tc1 ($2.33 \pm 0.89\%$ IA/g) and Tc2 ($2.63 \pm 0.50\%$ IA/g) at 1 h p.i.

Furthermore, Tc1 and Tc2 showed a similar and unfavorable biodistribution profile, with slow clearance from the bloodstream and a very low overall excretion from whole animal body as only 21.4 and 27.7% of total activity, respectively, was eliminated after 4 h p.i. Although some excretion occurred by a renal excretion route, the hepatobiliary excretion pathway played a prominent role, as seen by high liver accumulation of Tc1 and Tc2 (30.4 ± 5.2 and $40.2 \pm 4.8\%$ IA/organ at 1 h p.i., for Tc1 and Tc2, respectively).

CONCLUSIONS

Novel cyclic α -MSH derivatives containing a thioether or an amino bridge were designed, conjugated to a bifunctional chelator through their C-terminus (L1 and L2), and used to prepare the respective Re and ^{99m}Tc tricarbonyl complexes (Re1/Tc1, Re2/Tc2). The peptide conjugates and their corresponding metalated derivatives displayed lower binding affinity for MC1R than the parent peptide (PG10N).

NMR structural analysis of the S-macrocycle family has shown that the peptide moiety always displayed an atypical β turn in comparison to cognate peptides, which present a well-defined type I (PG10N) or type II β turn (MTII) in solution. The

radiopeptides presented significant cell internalization and moderate retention in murine melanoma cells. Biodistribution studies in melanoma-bearing mice showed that both are stable in vivo; however, their tumor-targeting properties are poor, correlating well with the low affinity of the rhenium surrogates.

MATERIALS AND METHODS

NDP-MSH was purchased from Neosystem (Strasbourg, France). Bovine serum albumin (BSA) was purchased from Sigma. Dulbecco's modified Eagle's medium (MEM) containing GlutaMax I, fetal bovine serum, penicillin/streptomycin antibiotic solution, trypsin-EDTA, and phosphate-buffered saline (PBS) pH 7.2 were all from Gibco-Invitrogen (Alfagene, Lisbon, Portugal). Fmoc-amino acids were obtained from CEM, while Fmoc-Asp(Dmab), Fmoc-Lys(ivDde), Rink Amide resin, and 2-(7-aza-1H-benzotriazole-1-yl)-1,1,3,3-tetramethyluronium hexafluorophosphate (HATU) were purchased from Novabiochem (Merck, Lisbon, Portugal). All other chemicals not specified were purchased from Aldrich. $\text{Na}^{99m}\text{TcO}_4$ was eluted from a $^{99}\text{Mo}/^{99m}\text{Tc}$ generator, using 0.9% saline. The IsoLink kit (Mallinckrodt-Covidien, Petten, The Netherlands) was used to prepare the radioactive precursor $\text{fac-}[^{99m}\text{Tc}(\text{CO})_3(\text{H}_2\text{O})_3]^+$ as described elsewhere.¹⁶ The synthon $\text{fac-}[\text{Re}(\text{CO})_3(\text{H}_2\text{O})_3]\text{Br}$ was also prepared according to a method described previously.¹⁷ No-carrier-added sodium [^{125}I]iodide (17.4 Ci/mg) in 0.1 M aqueous NaOH was obtained from Perkin-Elmer-Life. The compounds 4-((2-(tert-butoxycarbonylamino)ethyl)(2-(3,5-dimethyl-1H-pyrazol-1-yl)ethyl)amino)butanoic acid (pz-(Boc)CO₂H) and $\text{fac-}[\text{Re}(\text{k}^3\text{-pz-CO}_2\text{H})(\text{CO})_3]^+$ were prepared as described elsewhere.^{9a,18}

Reverse-Phase High-Performance Liquid Chromatography (RP-HPLC) Analysis. RP-HPLC was performed using a Perkin-Elmer system (LCPump, Series 200) coupled to a UV-vis detector (LC 290, Perkin-Elmer or SDP-10AV, Shimadzu) and a γ detector (LB 507 or LB 509, Berthold) for the ^{99m}Tc compounds. Analytical and semipreparative purification of the peptide conjugates was achieved on a Machery-Nagel column (250/4 mm, 10 μm) and Machery-Nagel column (250/8 mm, 7 μm), respectively. The contents of the columns were eluted with a binary gradient system with a flow rate of 1.0 mL/min (analytical) or 2.0 mL/min (semipreparative) using the following mobile phases: mobile phase A, TFA 0.1%; mobile phase B, CH₃CN 0.1% TFA. The method for the analytical control and semipreparative purification of the peptide conjugates was as follows: 0–35 min, 20–60% B; 35–37 min, 60% B; 37–38 min, 60–20% B; 38–40 min, 20% B. For all RP-HPLC methods presented, the absorbance was monitored at 220 and 280 nm.

Analytical separations were achieved on a Hypersil ODS column (250 \times 4 mm, 10 μm), and semipreparative separations of the radioactive complexes were achieved on a Hypersil ODS column (250 \times 8 mm, 10 μm). The contents of the columns were eluted with a binary gradient system with a flow rate of 1.0 mL/min (analytical) or 3.0 mL/min

Table 6. Biodistribution of Tc1 and Tc2 in B16F1 Melanoma-Bearing C57BL/6 Mice at 1 and 4 h p.i. (iv)^a

	Tc1		Tc2	
	1 h	4 h	1 h	4 h
	Tissues (% IA/g)			
tumor	2.33 ± 0.89	1.38 ± 0.18	2.63 ± 0.50	2.47 ± 0.70
blood	3.8 ± 1.1	2.6 ± 1.2	8.0 ± 1.0	3.9 ± 0.2
liver	29.8 ± 4.6	30.9 ± 4.2	40.2 ± 4.8	24.3 ± 1.7
intestine	7.2 ± 1.5	11.7 ± 3.1	5.8 ± 1.2	10.5 ± 1.1
spleen	3.3 ± 2.2	4.6 ± 3.9	7.5 ± 0.6	5.1 ± 0.3
heart	2.2 ± 0.3	1.3 ± 0.2	3.8 ± 0.3	2.0 ± 0.3
lung	4.7 ± 0.5	3.0 ± 2.0	8.8 ± 0.7	4.7 ± 0.2
kidney	23.2 ± 2.4	10.0 ± 3.3	18.4 ± 2.1	9.7 ± 1.1
muscle	0.5 ± 0.1	0.18 ± 0.16	0.67 ± 0.06	0.41 ± 0.08
bone	1.1 ± 0.4	0.45 ± 0.37	1.9 ± 0.2	1.5 ± 0.3
stomach	2.4 ± 0.6	1.5 ± 0.9	2.7 ± 1.0	1.0 ± 0.2
pancreas	2.0 ± 1.3	2.5 ± 2.5	1.1 ± 0.1	1.0 ± 0.1
	Uptake Ratio of Tumor to Normal Tissue and Total Excretion (%)			
tumor/blood	0.61	0.53	0.33	0.63
tumor/muscle	4.7	7.7	3.9	6.0
tumor/kidney	0.10	0.14	0.14	0.25
total excretion	10.8 ± 9.5	21.4 ± 4.6	13.0 ± 1.1	27.7 ± 1.3

^aThe data are presented as percent injected activity/gram of tissue (%IA/g) (mean ± SD, *n* = 3, 4).

(semipreparative) using the following mobile phases: mobile phase A, 0.5% TFA; mobile phase B, CH₃CN 0.5% TFA. The method for the analytical control of the conjugates L1 and L2 and radioconjugates Tc1 and Tc2 as well as the metalated conjugates Re1 and Re2 was as follows: 0–18 min, 15–100% B; 18–20 min, 100–15% B; 20–30 min, 15% B. Analytical control of the conjugates 3 was achieved on Symmetry C18 (250 × 4.6 mm) with a flow rate of 1 mL/min, using the following mobile phases and method: mobile phase A, TFA 0.1%; mobile phase B, CH₃CN 0.1% TFA; method, 0–30 min, 20–80% (210 nm).

The method for the semipreparative separation of the cyclic radioconjugate was as follows: 0–15 min, 15–30% B; 15–30 min, 30% B; 30–45 min 30–60% B, 45–60 min 60% B.

Peptide Synthesis. The peptides c[S-NO₂-C₆H₃-CO-His-DPhe-Arg-Trp-Cys]-Lys-NH₂ (1) and c[NH-NO₂-C₆H₃-CO-His-DPhe-Arg-Trp-Lys]-Lys-NH₂ (2) were prepared by following the modified procedures from the literature.⁸ Briefly, the peptide linear sequences NH₂-His(Trt)-DPhe-Arg(Pbf)-Trp(Boc)-Cys(Trt)-Lys(Boc)-NH₂ and NH₂-His(Trt)-DPhe-Arg(Pbf)-Trp(Boc)-Lys(Mtt)-Lys(Boc)-NH₂ were assembled to the MBHA rink Amide resin by Fmoc-based solid-phase peptide synthesis in a CEM 12-channel automated peptide synthesizer using HOBT/HBTU as coupling agents. The peptides were capped with fluoronitrobenzoic acid as previously reported, and before the cyclization step, the S-Trt group of the Cys residue was removed with dilute TFA (5% in CH₂Cl₂) without cleavage of the peptide from the resin. The cyclization step was carried out by treating the supported peptides with 5 equiv of K₂CO₃ in DMF at 25 °C with gentle shaking for 36 h. The peptide resin was washed with DMF (2×), H₂O (3×), DMF (3×), H₂O (2×), CH₃OH (3×), and CH₂Cl₂ (3×) and then vacuum-dried. The peptides were cleaved from the resin by treatment with a mixture of 95% TFA, 2.5% TIS, and 2.5% H₂O (5 mL) for 2 h. The cleavage solution was separated from the resin by filtration and concentrated under N₂. The crude peptide was precipitated and washed with ethyl ether, vacuum-dried, and dissolved in H₂O before lyophilization. After semipreparative purification and evaporation of solvents from the corresponding fractions, peptides 1 and 2 were obtained as yellow and pale green solids, respectively. Peptide 1, c[S-NO₂-C₆H₃-CO-His-DPhe-Arg-Trp-Cys]-Lys-NH₂ (mol wt C₄₈H₅₉N₁₅O₉S 1021.5): calcd *m/z* for [M + H]⁺ 1022.5, found 1022.5, *t*_R = 9.1 min. Peptide 2, c[NH-NO₂-C₆H₃-CO-His-DPhe-Arg-Trp-Lys]-Lys-NH₂ (mol wt C₅₁H₆₆N₁₆O₉ 1047.1): calcd *m/z* for [M + 2H]²⁺ 524.5, found 524.5, *t*_R = 9.3 min.

Synthesis of Peptide Derivatives. The derivatives L1, L2, Re1, and Re2 were prepared using the following procedure: pz-CO₂H

(2.5 equiv) or rhenium complex *fac*-[Re(CO)₃(κ³-pz-CO₂H)]⁺ (2.5 equiv) preincubated for 30 min with HATU (1.1 equiv. relative to the carboxylic group) was added to the peptide (ca. 800 μg) dissolved in *N,N*-diisopropylethylamine (20 μL)/dimethylformamide (250 μL). The pH was adjusted to 7–8 using DIPEA, and the reaction mixture was stirred at room temperature for 3 h. The crude products were purified by semipreparative RP-HPLC. After solvent evaporation, Boc deprotection of the peptides was achieved with a standard cocktail (95% TFA, 2.5% TIS, 2.5% H₂O). The compounds were precipitated with ice-cold diethyl ether, dried under a stream of nitrogen, and lyophilized. Compounds L1, Re1, L2, and Re2 were characterized by electrospray ionization-mass spectrometry (ESI-MS) and RP-HPLC. c[S-NO₂-C₆H₃-CO-His-DPhe-Arg-Trp-Cys]-Lys(pz)-NH₂ (L1): calcd *m/z* for [M + H]⁺ 1272.5, found 1272.5, *t*_R = 16.6 min. c[S-NO₂-C₆H₃-CO-His-DPhe-Arg-Trp-Lys]-Lys(pz)-NH₂ (L2): calcd *m/z* for [M + H]⁺ 1297.7, found 1297.7, *t*_R = 16.8 min. c[S-NO₂-C₆H₃-CO-His-DPhe-Arg-Trp-Cys]-Lys(pz-Re(CO)₃)-NH₂ (Re1): calcd *m/z* for [M + 2H]⁺ 772.2, found 772.2, *t*_R = 20.3 min. c[S-NO₂-C₆H₃-CO-His-DPhe-Arg-Trp-Lys]-Lys(pz-Re(CO)₃)-NH₂ (Re2): calcd *m/z* for [M + 2H]²⁺ 784.8, found 784.4, *t*_R = 21.0 min.

Thin-Layer Chromatography Analysis. Thin-layer chromatography (TLC) was performed using silica gel TLC strips (Polygram Sil G, Macherey-Nagel) developed with a mobile phase of 5% 6 N HCl in methanol.

Radioactivity detection was performed on a radiochromatograph (Berthold LB 2723) equipped with a 20 mm diameter NaI(Tl) scintillation crystal.

NMR Spectroscopy of Peptides 1, L1, and Re1. Samples for NMR spectra acquisition at approximately 1 mM peptide concentration were prepared by dissolving the lyophilized compounds (~0.5 mg) in 0.5 mL of H₂O/D₂O (9/1 v/v). The pH was adjusted to 2.5 by adding minimal amounts of NaOD or DCl, measured with a glass micro electrode and not corrected for isotope effects. Sodium 2,2-dimethyl-2-silapentane-5-sulfonate (DSS) was used as an internal reference.

NMR spectra were acquired at 5 and 25 °C on a Bruker AV-600 spectrometer operating at a proton frequency of 600.13 MHz and equipped with a cryoprobe. The temperature of the NMR probe was calibrated using a methanol sample. 1D spectra were acquired using 32 K data points, which were zero-filled to 64 K data points before performing the Fourier transformation. As previously reported,¹⁹ 2D spectra, i.e., phase-sensitive correlated spectroscopy (COSY), total correlated spectroscopy (TOCSY), nuclear Overhauser enhancement spectroscopy (NOESY), and rotating frame nuclear Overhauser spectroscopy

(ROESY), were recorded by standard techniques using presaturation of the water signal and the time-proportional phase incrementation mode. NOESY and ROESY mixing times were 150 and 200 ms, respectively. TOCSY spectra were acquired using 60 ms DIPSI2 with a z filter spin-lock sequence. ^1H - ^{13}C and ^1H - ^{15}N heteronuclear single quantum coherence spectra (HSQC) were recorded at natural heteronuclear abundance. Acquisition data matrices were defined by 2048×512 (128 in the case of the ^1H - ^{15}N HSQC spectrum) points in t_2 and t_1 , respectively. Data were processed using the standard TOPSPIN program.²⁰ The 2D data matrix was multiplied by either a square-sine-bell or a sine-bell window function with the corresponding shift optimized for every spectrum and zero-filled to a $2\text{K} \times 1\text{K}$ (256 points in the ^1H - ^{15}N HSQC) complex matrix prior to Fourier transformation. Baseline correction was applied in both dimensions. The 0 ppm ^{13}C and ^{15}N δ values were obtained indirectly by multiplying the spectrometer frequency that corresponds to 0 ppm in the ^1H spectrum, assigned to internal DSS reference, by 0.251 449 53 and 0.101 329 118, respectively.²¹

NMR Assignment. ^1H NMR signals of peptide **1** and the peptide moiety in **L1** and **Re1** were assigned by standard sequential assignment methods.²² Then, the ^{13}C and ^{15}N resonances were straightforwardly assigned from the cross-correlations observed in the corresponding HSQC spectra between the proton and the bound carbon or nitrogen, respectively.

The chelator resonances in the peptide conjugates **L1** and **Re1** were assigned by the combined analysis of 2D COSY, TOCSY, NOESY, and ^1H , ^{13}C -HSQC spectra, taking into account previous NMR assignments for the isolated chelator.²³

NMR Structure Calculation. The peak lists for the NOESY and ROESY spectra of peptide **1** were generated by interactive peak picking and the peak volumes obtained by the automatic integration function of Sparky.²⁴ The three-dimensional structure was calculated using torsion angle dynamics²⁵ implemented in the program CYANA.²⁶ The applied CYANA protocol consisted of seven iterative cycles of automatic NOE assignment and structure calculation, followed by a final standard structure calculation.

Furthermore, a negative value for the torsion angle ψ for L-amino acids and the distance constraints required for cyclization between Cys6 and the $-\text{NO}_2\text{-C}_6\text{H}_3\text{-CO-}$ linker were used during the NOE assignment/structure calculation cycles. In each cycle, the structure calculation started from 100 randomized conformers and the standard CYANA-simulated annealing schedule²⁵ was used with 10 000 torsion angle dynamics steps per conformer.

MOLMOL²⁷ was used to visualize and analyze the final structures.

Cell Culture. B16F1 murine melanoma cells (ECACC, Salisbury, U.K.) were grown in MEM containing GlutaMax I supplemented with 10% heat-inactivated fetal bovine serum and 1% penicillin/streptomycin antibiotic solution (all from Gibco-Invitrogen). Cells were cultured in a humidified atmosphere of 95% air and 5% CO_2 at 37 °C (Heraeus, Hanau, Germany), with the medium changed every other day. The cells were adherent in monolayers and, when confluent, were harvested from the cell culture flasks with trypsin EDTA (Gibco-Invitrogen) and seeded further apart.

Radioiodination. Radioiodination of NDP- α -MSH was performed as described in the literature with a small modification.²⁸ Briefly, 10 μL of Na^{125}I (1.5 mCi) and 10 μL of chloramine-T solution (50 mg/25 mL of PBS, 0.3 M) were added to 5 μL of NDP- α -MSH solution (5 μg of peptide/50 μL of PBS 0.3 M). After 5 min of incubation at room temperature with shaking, the reaction was stopped by addition of dithiothreitol (10 mg) and BSA (100 μL) to the solution. The reaction mixture was loaded onto a small reverse-phase cartridge (Sep-Pak C18, Waters), which was washed consecutively with methanol and 0.1% TFA aqueous solution (0.1% TFA), and finally the iodinated peptide was eluted with methanol and collected. The fractions containing [^{125}I]NDP-MSH were stored at -20 °C. Preceding each binding experiment, an additional purification was performed by RP-HPLC.

Competitive Binding Assay. The inhibitory concentration of 50% (IC_{50}) values for the α -MSH analogues were determined by competitive binding assays with [^{125}I]NDP- α -MSH in B16F1 melanoma cells. Cells were harvested, seeded into 24-well cell culture plates (2×10^5 cells/well),

and allowed to attach overnight. After they were washed once with the binding medium (0.3 mL, MEM with 25 mM HEPES and 0.2% BSA), the cells were incubated at room temperature (25 °C) for 2 h with the competitor peptide solution (0.1 mL), yielding a final concentration ranging from 1×10^{-5} to 1×10^{-12} M, and [^{125}I]NDP- α -MSH (50 000 cpm in 0.2 mL). The reaction media was then removed, and the cells were washed twice with cold 0.01 M PBS pH 7.2 with 0.2% of BSA (0.5 mL) and lysed with NaOH 1 M (0.5 mL) for 5 min. The radioactivity of the lysate was measured in a γ counter. The competitive binding curves were obtained by plotting the percentage of [^{125}I]NDP- α -MSH bound to the cells vs concentrations of displacing peptides. IC_{50} values for the peptides were calculated by using GraphPad Prism software. All cell binding experiments were carried out in triplicate.

Radiolabeling with $^{99\text{m}}\text{Tc}(\text{I})$. $\text{Na}^{[99\text{m}}\text{TcO}_4]$ was eluted from a $^{99}\text{Mo}/^{99\text{m}}\text{Tc}$ generator, using 0.9% saline. The precursor $\text{fac-}^{[99\text{m}}\text{Tc}(\text{CO})_3(\text{H}_2\text{O})_3]^+$ was prepared using an Isolink kit (Coviden, formerly Mallinckrodt) and its radiochemical purity monitored by RP-HPLC.

Compounds **Tc1** and **Tc2** were obtained by reacting **L1** and **L2** with $\text{fac-}^{[99\text{m}}\text{Tc}(\text{CO})_3(\text{H}_2\text{O})_3]^+$, respectively. Briefly, a solution of $\text{fac-}^{[99\text{m}}\text{Tc}(\text{CO})_3(\text{H}_2\text{O})_3]^+$ (900 μL) was added to a capped vial, previously flushed with N_2 , containing **L1** or **L2** (100 μL , 5×10^{-4} M). The mixture reacted for 30 min at 98 °C, and the radiochemical purity of **Tc1** and **Tc2** was checked by RP-HPLC, using an analytical C-18 reversed-phase column. The radiolabeled compound was purified by semipreparative RP-HPLC. The activity corresponding to $^{99\text{m}}\text{Tc}(\text{CO})_3$ -peptide conjugates was collected in 50 mL Falcon vials containing 200 μL of PBS for biodistribution and cell internalization studies. The solutions were concentrated to a final volume of 200 μL under a nitrogen stream, and the product was controlled by analytical RP-HPLC to confirm its purity and stability after purification and evaporation.

Partition Coefficient. The partition coefficient was evaluated by the "shake-flask" method.²⁹ The radioconjugate was added to a mixture of octanol (1 mL) and 0.1 M PBS (pH 7.4; 1 mL), which had been previously saturated with each other by stirring. This mixture was vortexed and centrifuged (3000 rpm, 10 min, room temperature) to allow phase separation. Aliquots of both octanol and PBS phases were counted in a γ counter. The partition coefficient ($P_{o/w}$) was calculated by dividing the counts in the octanol phase by those in the buffer, and the results were expressed as $\log P_{o/w}$.

In Vitro Stability. The $^{99\text{m}}\text{Tc}$ -labeled complex (100 μL , ~ 10 MBq) was added to fresh human plasma (1 mL), and the mixture was incubated at 37 °C. At appropriate time points (2, 4, and 6 h), 100 μL aliquots (in duplicate) were sampled and treated with 200 μL of ethanol to precipitate the proteins. Samples were centrifuged at 3000 rpm for 15 min at 4 °C, and the supernatant was analyzed by HPLC. The stability of the radiolabeled conjugate in the solutions containing 0.2% BSA was checked by RP-HPLC using the chromatographic methods previously described and by instant thin-layer chromatography.

Internalization and Cellular Retention Studies. Internalization assays of the radiopeptides were performed in B16F1 murine melanoma cells seeded at a density of 0.2 million per well in plates and allowed to attach overnight. The cells were incubated at 37 °C for a period of 5 min to 4 h with about 200 000 cpm of the conjugate in 0.5 mL of assay medium (MEM with 25 mM *N*-(2-hydroxyethyl)piperazine-*N*-ethanesulfonic acid and 0.2% BSA). Incubation was terminated by washing the cells with ice-cold assay medium. Cell-surface-bound radioligand was removed by two steps of acid wash (50 mM glycine, HCl/100 mM NaCl, pH 2.8) at room temperature for 5 min. The pH was neutralized with cold PBS with 0.2% BSA, and subsequently the cells were lysed by 10 min incubation with 1 M NaOH at 37 °C to determine the internalized radioligand. The cellular retention properties of the internalized radioconjugates were determined by incubating B16F1 cells with the radiolabeled compound for 2 h at 37 °C, washing them with cold assay medium, removing the membrane-bound radioactivity with acid buffer wash, and monitoring radioactivity release into the culture media (0.5 mL) at 37 °C. At different time points over a 4 h incubation period, the radioactivity in the medium and that in the cells were separately collected and counted.

Biodistribution. All animal experiments were performed in compliance with national and European regulations for animal

treatment. The animals were housed in a temperature- and humidity-controlled room with a 12 h light/12 h dark schedule. Biodistribution of the radiolabeled complex (2.6–3.7 GBq) diluted in 100 μ L of PBS pH 7.2. Mice ($n = 3–5$ per time point) were killed by cervical dislocation at 1 and 4 h after injection. The dose administered and the radioactivity in the killed animals were measured using a dose calibrator (Curiometer IGC-3, Aloka, Tokyo, Japan or Capintec CRC-15W, Ramsey, USA). The difference between the radioactivity in the injected animals and that in the killed animals was assumed to be due to excretion. Tumors and normal tissues of interest were dissected, rinsed to remove excess blood, and weighed, and their radioactivity was measured using a γ counter (LB2111, Berthold, Germany). The uptake in the tumor and healthy tissues of interest was calculated and expressed as a percentage of the injected radioactivity dose per gram of tissue. For blood, bone, muscle, and skin, total activity was estimated assuming that these organs constitute 6, 10, 40, and 15% of the total body weight, respectively. Urine was also collected and pooled together at the time the animals were killed.

■ ASSOCIATED CONTENT

■ Supporting Information

Tables and figures giving ^1H , ^{13}C , and ^{15}N chemical shifts, representative NOEs, coupling constants, and deviation from the random coil structure for **1**, **LI**, and **Re1**, respectively. This material is available free of charge via the Internet at <http://pubs.acs.org>.

■ AUTHOR INFORMATION

Notes

The authors declare no competing financial interest.

■ ACKNOWLEDGMENTS

M.M. thanks the Fundação para a Ciência e Tecnologia (FCT) for a Ph.D. fellowship (SFRH/BD/48066/2008). Covidien-Mallinckrodt is acknowledged for the IsoLink kits. J. Marçalo is acknowledged for performing the ESI-MS analyses. The electrospray ionization quadrupole ion trap mass spectrometer was acquired with the support of the Programa Nacional de Reequipamento Científico of the FCT, which is part of the RNEM-Rede Nacional de Espectrometria de Massa, also supported by the FCT. D.P.-U. and M.A.J. thank the Spanish MICINN project CTQ2011-22514 for financial support.

■ REFERENCES

(1) (a) Correia, J. D.; Paulo, A.; Raposinho, P. D.; Santos, I. Radiometallated peptides for molecular imaging and targeted therapy. *Dalton Trans.* **2011**, 40 (23), 6144–6167. (b) Reubi, J. C.; Maecke, H. R. Peptide-based probes for cancer imaging. *J. Nucl. Med.* **2008**, 49 (11), 1735–1738. (c) Jamal, A.; Siegel, R.; Xu, J. Q.; Ward, E. Cancer Statistics. *Ca-Cancer J. Clin.* **2010**, 60 (5), 277–300. (d) Lee, S.; Xie, J.; Chen, X. Peptide-based probes for targeted molecular imaging. *Biochemistry* **2010**, 49 (7), 1364–1376.

(2) Miao, Y.; Quinn, T. P. Peptide-targeted radionuclide therapy for melanoma. *Crit. Rev. Oncol. Hematol.* **2008**, 67 (3), 213–228.

(3) (a) Gray-Schopfer, V.; Wellbrock, C.; Marais, R. Melanoma biology and new targeted therapy. *Nature* **2007**, 445 (7130), 851–857. (b) Carlson, J. A.; Slominski, A.; Linette, G. P.; Mihm, M. C., Jr.; Ross, J. S. Biomarkers in melanoma: staging, prognosis and detection of early metastases. *Expert Rev. Mol. Diagn.* **2003**, 3 (3), 303–330. (c) Carlson, J. A.; Slominski, A.; Linette, G. P.; Mihm, M. C., Jr.; Ross, J. S. Biomarkers

in melanoma: predisposition, screening and diagnosis. *Expert Rev. Mol. Diagn.* **2003**, 3 (2), 163–184.

(4) Raposinho, P. D.; Correia, J. D. G.; Oliveira, M. C.; Santos, I. Melanocortin-1 Receptor-Targeting With Radiolabeled Cyclic α -Melanocyte-Stimulating Hormone Analogs for Melanoma Imaging. *Biopolymers* **2010**, 94 (6), 820–829.

(5) (a) Haskell-Luevano, C.; Todorovic, A.; Gridley, K.; Sorenson, N.; Irani, B.; Xiang, Z. The melanocortin pathway: effects of voluntary exercise on the melanocortin-4 receptor knockout mice and ACTH(1–24) ligand structure activity relationships at the melanocortin-2 receptor. *Endocr. Res.* **2004**, 30 (4), 591–597. (b) Holder, J. R.; Haskell-Luevano, C. Melanocortin ligands: 30 years of structure-activity relationship (SAR) studies. *Med. Res. Rev.* **2004**, 24 (3), 325–356. (c) Garcia-Borrón, J. C.; Sanchez-Laorden, B. L.; Jimenez-Cervantes, C. Melanocortin-1 receptor structure and functional regulation. *Pigment Cell Res.* **2005**, 18 (6), 393–410.

(6) (a) Al-Obeidi, F.; Castrucci, A. M.; Hadley, M. E.; Hrubby, V. J. Potent and prolonged acting cyclic lactam analogues of α -melanotropin: design based on molecular dynamics. *J. Med. Chem.* **1989**, 32 (12), 2555–2561. (b) Dorr, R. T.; Lines, R.; Levine, N.; Brooks, C.; Xiang, L.; Hrubby, V. J.; Hadley, M. E. Evaluation of melanotan-II, a superpotent cyclic melanotropic peptide in a pilot phase-I clinical study. *Life Sci.* **1996**, 58 (20), 1777–1784.

(7) (a) Hrubby, V. J.; Lu, D.; Sharma, S. D.; Castrucci, A. L.; Kesterson, R. A.; al-Obeidi, F. A.; Hadley, M. E.; Cone, R. D. Cyclic lactam α -melanotropin analogues of Ac-Nle⁴-cyclo[Asp⁵,D-Phe⁷,Lys¹⁰] α -melanocyte-stimulating hormone-(4–10)-NH₂ with bulky aromatic amino acids at position 7 show high antagonist potency and selectivity at specific melanocortin receptors. *J. Med. Chem.* **1995**, 38 (18), 3454–3461. (b) Nijenhuis, W. A. J.; Wanders, N.; Kruijtzter, J. A. W.; Liskamp, R. M.; Gispen, W. H.; Adan, R. A. H. Accelerating sensory recovery after sciatic nerve crush: non-selective versus melanocortin MC4 receptor-selective peptides. *Eur. J. Pharmacol.* **2004**, 495 (2–3), 145–152. (c) Mayorov, A. V.; Han, S. Y.; Cai, M.; Hammer, M. R.; Trivedi, D.; Hrubby, V. J. Effects of macrocycle size and rigidity on melanocortin receptor-1 and -5 selectivity in cyclic lactam α -melanocyte-stimulating hormone analogs. *Chem. Biol. Drug Des.* **2006**, 67 (5), 329–335.

(8) Grieco, P.; Cai, M.; Liu, L.; Mayorov, A.; Chandler, K.; Trivedi, D.; Lin, G.; Campiglia, P.; Novellino, E.; Hrubby, V. J. Design and microwave-assisted synthesis of novel macrocyclic peptides active at melanocortin receptors: discovery of potent and selective hMCSR receptor antagonists. *J. Med. Chem.* **2008**, 51 (9), 2701–2707.

(9) (a) Alves, S.; Paulo, A.; Correia, J. D. G.; Gano, L.; Smith, C. J.; Hoffman, T. J.; Santos, I. Pyrazolyl derivatives as bifunctional chelators for labeling tumor-seeking peptides with the *fac*-[M(CO)₃]⁺ moiety (M = ^{99m}Tc, Re): Synthesis, characterization, and biological behavior. *Bioconjugate Chem.* **2005**, 16 (2), 438–449. (b) Correia, J. D.; Paulo, A.; Santos, I. Re and Tc Complexes with Pyrazolyl-Containing Chelators: from Coordination Chemistry to Target-Specific Delivery of Radioactivity. *Curr. Radiopharm.* **2009**, 2 (4), 277–294.

(10) (a) Alves, S.; Correia, J. D. G.; Santos, I.; Veerendra, B.; Sieckman, G. L.; Hoffman, T. J.; Rold, T. L.; Figueroa, S. D.; Retzlöff, L.; McCrate, J.; Prasanphanich, A.; Smith, C. J. Pyrazolyl conjugates of bombesin: a new tridentate ligand framework for the stabilization of *fac*-[M(CO)₃]⁺ moiety. *Nucl. Med. Biol.* **2006**, 33 (5), 625–634. (b) Raposinho, P. D.; Correia, J. D. G.; Alves, S.; Botelho, M. F.; Santos, A. C.; Santos, I. A ^{99m}Tc(CO)₃-labeled pyrazolyl- α -melanocyte-stimulating hormone analog conjugate for melanoma targeting. *Nucl. Med. Biol.* **2008**, 35 (1), 91–99. (c) Raposinho, P. D.; Xavier, C.; Correia, J. D. G.; Falcao, S.; Gomes, P.; Santos, I. Melanoma targeting with α -melanocyte stimulating hormone analogs labeled with *fac*-[^{99m}Tc(CO)₃]⁺: effect of cyclization on tumor-seeking properties. *J. Biol. Inorg. Chem.* **2008**, 13 (3), 449–459.

(11) Grieco, P.; Campiglia, P.; Gomez-Monterrey, I.; Lama, T.; Novellino, E. Rapid and efficient methodology to perform macrocyclization reactions in solid-phase peptide chemistry. *Synlett* **2003**, 14, 2216–2218.

- (12) (a) Oliveira, B. L.; Correia, J. D.; Raposinho, P. D.; Santos, I.; Ferreira, A.; Cordeiro, C.; Freire, A. P. Re and (99m)Tc organometallic complexes containing pendant l-arginine derivatives as potential probes of inducible nitric oxide synthase. *Dalton Trans.* **2009**, *1*, 152–162. (b) Simpson, E. J.; Hickey, J. L.; Breadner, D.; Luyt, L. G. Investigation of isomer formation upon coordination of bifunctional histidine analogues with $^{99m}\text{Tc}/\text{Re}(\text{CO})_3$. *Dalton Trans.* **2012**, *41* (10), 2950–2958. (c) Perera, T.; Marzilli, P. A.; Fronczek, F. R.; Marzilli, L. G. Several novel N-donor tridentate ligands formed in chemical studies of new *fac*- $\text{Re}(\text{CO})_3$ complexes relevant to *fac*- $^{99m}\text{Tc}(\text{CO})_3$ radiopharmaceuticals: attack of a terminal amine on coordinated acetonitrile. *Inorg. Chem.* **2010**, *49* (5), 2123–2131.
- (13) Elipe, M. V. S.; Mosley, R. T.; Bednarek, M. A.; Arison, B. H. H-1-NMR studies on a potent and selective antagonist at human melanocortin receptor 4 (hMC-4R). *Biopolymers* **2003**, *68* (4), 512–527.
- (14) Cho, M. K.; Lee, C. J.; Lee, C. H.; Li, S. Z.; Lim, S. K.; Baik, J. H.; Lee, W. Structure and function of the potent cyclic and linear melanocortin analogues. *J. Struct. Biol.* **2005**, *150* (3), 300–308.
- (15) Ying, J.; Kover, K. E.; Gu, X.; Han, G.; Trivedi, D. B.; Kavarana, M. J.; Hruby, V. J. Solution structures of cyclic melanocortin agonists and antagonists by NMR. *Biopolymers* **2003**, *71* (6), 696–716.
- (16) Alberto, R.; Ortner, K.; Wheatley, N.; Schibli, R.; Schubiger, A. P. Synthesis and properties of boranocarbonate: a convenient in situ CO source for the aqueous preparation of $[\text{}^{99m}\text{Tc}(\text{OH}_2)_3(\text{CO})_3]^+$. *J. Am. Chem. Soc.* **2001**, *123* (13), 3135–3136.
- (17) Zubieta, J.; Lazarova, N.; James, S.; Babich, J. A convenient synthesis, chemical characterization and reactivity of $[\text{Re}(\text{CO})_3(\text{H}_2\text{O})_3]\text{Br}$: the crystal and molecular structure of $[\text{Re}(\text{CO})_3(\text{CH}_3\text{CN})_2\text{Br}]$. *Inorg. Chem. Commun.* **2004**, *7* (9), 1023–1026.
- (18) Morais, M.; Raposinho, P. D.; Oliveira, M. C.; Correia, J. D.; Santos, I. Evaluation of novel $^{99m}\text{Tc}(\text{I})$ -labeled homobivalent alpha-melanocyte-stimulating hormone analogs for melanocortin-1 receptor targeting. *J. Biol. Inorg. Chem.* **2012**, *4*, 491–505.
- (19) Mirassou, Y.; Santiveri, C. M.; de Vega, M. J. P.; Gonzalez-Muniz, R.; Jimenez, M. A. Disulfide Bonds versus Trp center dot center dot center dot Trp Pairs in Irregular beta-Hairpins: NMR Structure of Vammin Loop 3-Derived Peptides as a Case Study. *ChemBioChem* **2009**, *10* (5), 902–910.
- (20) *TOPSPIN, p., NMR Data Acquisition and Processing Software*; Bruker Biospin, Karlsruhe, Germany.
- (21) Wishart, D. S.; Bigam, C. G.; Yao, J.; Abildgaard, F.; Dyson, H. J.; Oldfield, E.; Markley, J. L.; Sykes, B. D. ^1H , ^{13}C and ^{15}N chemical shift referencing in biomolecular NMR. *J. Biomol. NMR* **1995**, *6* (2), 135–140.
- (22) Wuthrich, K. *NMR of proteins and nucleic acids*; Wiley: New York, 1986.
- (23) Palma, E.; Oliveira, B. L.; Correia, J. D. G.; Gano, L.; Maria, L.; Santos, I. C.; Santos, I. A new bisphosphonate-containing $^{99m}\text{Tc}(\text{I})$ tricarbonyl complex potentially useful as bone-seeking agent: synthesis and biological evaluation. *J. Biol. Inorg. Chem.* **2007**, *12* (5), 667–679.
- (24) Goddard, T. D.; Kneller, D. G. *SPARKY 3*; University of California, San Francisco, 1999.
- (25) Guntert, P.; Mumenthaler, C.; Wuthrich, K. Torsion angle dynamics for NMR structure calculation with the new program DYANA. *J. Mol. Biol.* **1997**, *273* (1), 283–298.
- (26) Güntert, P. Automated NMR Protein Structure Calculation. *Prog. Nucl. Magn. Reson. Spectrosc.* **2003**, *43*, 105.
- (27) Koradi, R.; Billeter, M.; Wuthrich, K. MOLMOL: a program for display and analysis of macromolecular structures. *J. Mol. Graph.* **1996**, *14* (1), 51–55.
- (28) Froidevaux, S.; Calame-Christe, M.; Tanner, H.; Eberle, A. N. Melanoma targeting with DOTA-alpha-melanocyte-stimulating hormone analogs: Structural parameters affecting tumor uptake and kidney uptake. *J. Nucl. Med.* **2005**, *46* (5), 887–895.
- (29) Troutner, D. E.; Volkert, W. A.; Hoffman, T. J.; Holmes, R. A. A neutral lipophilic complex of ^{99m}Tc with a multidentate amine oxime. *Int. J. Appl. Radiat. Isot.* **1984**, *35* (6), 467–470.